The Journal of Chemical Physics ARTICLE pubs.aip.org/aip/jcp

# Response of a 4-nitrothiophenol monolayer to rapid heating studied by vibrational sum frequency spectroscopy

Cite as: J. Chem. Phys. 161, 194711 (2024); doi: 10.1063/5.0231489
Submitted: 31 July 2024 • Accepted: 1 November 2024 •
Published Online: 19 November 2024



Matthias Linke, Joshua Multhaup,[a] and Eckart Hasselbrink[b]

## AFFILIATIONS

Fakultät für Chemie and Center for Nanointegration (CENIDE), Universität Duisburg-Essen, D-45117 Essen, Germany

**Note:** This paper is part of the JCP Festschrift in Honor of Yuen-Ron Shen.
[a]**Present address:** Chemistry Department, Dartmouth College, 03755-NH Hanover, USA.
[b]**Author to whom correspondence should be addressed:** Eckart.Hasselbrink@Uni-Duisburg-Essen.de.

## ABSTRACT

A monolayer of 4-nitrothiophenol adsorbed on an Au substrate was heated by illuminating the substrate with a 19 ps laser pulse of 532 nm wavelength. Within 91 ps, the temperature of the sample increased from room temperature by 113 K. Vibrational sum frequency spectroscopy was used to characterize the adsorption geometry of the molecules in the ordered domains in the monolayer film. Upon heating, the initially ordered monolayer largely lost its structure. While the molecules are initially tilted by about 50° with respect to the surface normal, the analysis indicates that the mean tilt angle increased to 80° with a spread for individual molecules of up to a tilt angle of 40° upon heating. The evolution of this loss of order lagged about 100 ps behind the temperature rise of the substrate.





## I. INTRODUCTION

Vibrational sum frequency spectroscopy (vSFS), to which Yuen-Ron Shen, as a pioneer,[1] has devoted most of his academic career, has over the last decades evolved to be the prime experimental tool for studying not only the static properties but also the dynamics of molecular systems at interfaces.[2] It is not only the inherent surface selectivity that grants it this dominant role, but further, it plays out to our advantage that the strict selection rules result in simpler spectra, particularly when studying well-ordered systems, such as self-assembled monolayers (SAMs) or Langmuir–Blodgett (LB) films.[3,4]

Energy transport across interfaces and in layered systems is a question of fundamental importance. Concepts that have been successfully applied at the engineering level may not provide insights at length scales of molecular dimensions, especially when temporarily sharp gradients exist that result from ultrafast energy impact. Energy flow in and between electronic and lattice degrees of freedom of materials with rigid structures, such as metals and inorganic semiconductors, has been studied intensively.[5–7] However, the literature is sparse when it comes to the energy transport along the axis of the molecules forming a monolayer between a solid substrate and air or vacuum. In seminal works, Wang and co-workers[8] have addressed this problem by utilizing an ultra-fast laser to heat the metallic substrate to a thiol monolayer and time-resolved vSFS to characterize the response. A small number of systems were then studied.[9,10] Molecular dynamics simulations have shed light on these dynamics from the theory side.[11,12]

In this paper, we report on the dynamics of a SAM of 4-nitrothiophenol (4-NTP) on a flat Au substrate. vSFS on the symmetric $NO_2$ stretch, the molecular group pointing away from the substrate, was used to gain insight into the temporal evolution of the order in the monolayer. A 19 ps long pulse of 532 nm light heats a thin metal film from the backside. Over the course of 91 ps, a temperature rise of ~113 K is induced at the surface, onto which the SAM is adsorbed. Under these conditions, hot electron mediated vibrational

excitation has a negligible effect. We present evidence that with a time lag of about 100 ps following the temperature increase in the Au substrate, the molecular order largely disappears. To this end, we exploit the possibility of analyzing vSF spectra obtained with different combinations of the polarization of the light beams involved to gain insight into the orientation of the adsorbed molecules. Our study differs insofar from earlier work, as the longer laser pulse length used for heating suppresses the influence of hot electron scattering events on the transient spectra, allowing us to better isolate the changes in conformational order and to quantify these.

## II. EXPERIMENTAL

A scanning vSF spectrometer with ~12 $cm^{-1}$ resolution was used (Ekspla PL2231 and PG501DFG) that utilizes tuneable IR and 532 nm light pulses of 19 ps duration at a repetition rate of 50 Hz. Pulse energies of 280 $\mu$J (532 nm) and 10–30 $\mu$J (IR) were employed. The 532 nm laser beam is split into two portions (50:50): one is used for upconversion in the vSFS, while the other is used to flash-heat the sample.

The polarization of the IR light is set using a $\lambda/2$-plate. Only *p* polarization is used for the experiment. The 532 nm light used for upconversion passes a combination of two Brewster type thin film polarizers and a $\lambda/2$-plate to control intensity and polarization. It was experimentally verified that the pulse energy of the 532 nm light did not change by more than 3% in the sample when switching from *s* to *p* polarization. The sum frequency (SF) light is directed by dielectric mirrors to the detector. This path introduced an error smaller than 3% in the detection efficiencies for *s* and *p* polarized light. The polarization of the SF light is defined by a polarizer placed in front of the photomultiplier registering the signal.

A sample stage was employed that permitted the direction of a laser beam at normal incidence onto the backside of the sample. Moreover, the sample was slowly rotated around its center normal and the probe spot placed off-center, such that, over time, different areas were utilized for the experiment. The IR and upconversion light beams were directed at the front of the sample under incident angles of 44° and 54°, respectively, and have surface spot sizes (FWHM) of 1.2 and 1.9 mm, respectively. A translation stage with 8 fs resolution was used to control the delay between the heating and probing laser pulses. For each data point, typically 361 laser pulses were sampled and averaged. As the experiments are required to record spectra at multiple delay line positions, it may take up to 24 h in total for one run. At each delay line position, a pair of spectra were recorded with the flash-heating laser pulse blocked and passing through a shutter. This allows us to rule out misleading effects from unaccounted degradation of the sample over the time of an experimental run.

The samples, 10 × 10 $mm^2$, were prepared at the local optics shop using commercially available glass cover slips (Menzel-Gläser 1, thickness 0.19–0.23 mm) as substrates, onto which first a 13 nm thick contact adhesion layer of Ti was deposited and then a 30 nm thick Au film. We settled on these two thicknesses after extensive testing as they provided stable systems, ensured that the Au film was closed, and resulted in a heat capacity small enough to allow us to obtain a significant temperature jump. Less than 10% of the 532 nm light penetrates from the backside through the film structure. Details of the monolayer preparation have been reported before.[13]

The spectra were fit using the following established expression:[14,15]

$$I^{SFS}(\omega_{IR}) \propto \left| \left|\chi^{(2)}_{NR}\right| + e^{i\xi} \frac{A_i}{\omega_{IR} - \omega + i\Gamma} \right|^2, \quad (1)$$

where $\chi^{(2)}_{NR}$ is the second order susceptibility leading to a non-resonant background. $A$, $\omega$, and $\Gamma$ are the vSF line strength, the position, and the width (HWHM) of the vibrational resonance, respectively. $\omega_{IR}$ is the frequency of the incident IR light. The parameters are real and always have a positive value in our model. $\xi$ is the phase difference between the non-resonant background and the molecular susceptibility. At 1342 $cm^{-1}$, the non-resonant background is relatively small in comparison to spectra recorded in the CH stretch region. Nevertheless, it causes a non-Lorentzian lineshape, indicating that the phase difference is not equal to $\pi/2$. It is worth noting that contributions from $\chi^{(3)}$ arising from the oriented dipole moments of the $NO_2$ groups are present, which similarly to a non-resonant background influence the lineshape.[16] However, this contribution cannot be quantified by us.

In this case, two distinct sets of fit parameters yield an identical spectrum.[17] However, by (*i*) recording the spectrum using the *ssp* and *ppp* polarization combinations, (*ii*) obtaining for both spectra all possible sets of fitting parameters, and (*iii*) comparing the predicted intensity ratios to calculated ones, we were able in a previous publication[13] to identify the correct parameter set. For further details, the reader is referred to the supplementary material.

The experiment requires a reading of the sample surface temperature with the time resolution of the laser system, namely, ~10 ps. Following earlier work in the literature, we used the change in reflectivity as a proxy for the temperature.[18] For this purpose, the reflected intensity of the 532 nm light used for upconversion was utilized. The measurement was calibrated by collecting data when the sample was stepwise heated from room temperature to 440 K. Part of the incoming light was reflected onto one photodiode, PD1, to monitor the intensity while another, PD2, recorded the intensity reflected from the sample. The normalized reflectivity change is then given by

$$\frac{\Delta R(T)}{R(0)} = \frac{R(T) - R_0}{R(0)} = \frac{\frac{PD_2(T)}{PD_1(T)} - \frac{PD_2(0)}{PD_1(0)}}{\frac{PD_2(0)}{PD_1(0)}} = \frac{PD_2(T)}{PD_1(T)} \frac{PD_1(0)}{PD_2(0)} - 1 = m\,\Delta T, \quad (2)$$

where $R(0)$ is the reflectivity at room temperature and $R(T)$ is the one at temperature $T$. A linear fit to the data obtains the slope $m$. The reflectivity change is for *s* polarized light only a 1/4 of that observed for *p*-polarized light. For this reason, only *p*-polarization was used for these measurements. The data from two such measurements using different samples are displayed in Fig. 1.

The data are well represented by a linear dependence, with a coefficient of 6.8 (3) × $10^{-4}$ $K^{-1}$ (Table I). Note that we subsequently always recorded the temperature concurrently with time-resolved spectra. For this purpose, a shutter blocking the flash-heat pulse could be closed. We expect the adsorption of a SAM to not significantly affect the surface reflectivity.

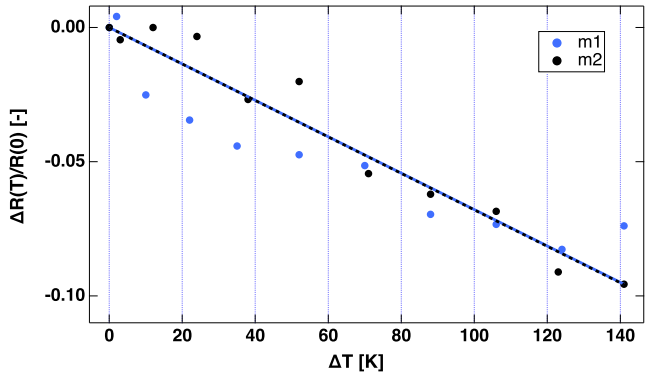


**FIG. 1.** Change in the surface reflectivity for *p* polarized light when elevating the temperature (static heating), recorded using two different samples. The straight lines are fits to the respective colors' data points. The vertical intercepts were fixed at 0. Data points with positive reflectivity changes were ignored when fitting. The slopes obtained were $-6.79 \times 10^{-4}$ K$^{-1}$ (black) and $-6.78 \times 10^{-4}$ K$^{-1}$ (blue).

**TABLE I.** Slopes and error margins of the thermoreflectivity calibration measurements on an Au(30 nm)/Ti(13 nm) sample.

| | Measurement | | |
|---|---|---|---|
| Fit parameter | m1 | m2 | $\overline{m}$ |
| Slope $m$ ($10^{-4}$ K$^{-1}$) | −6.79 | −6.78 | −6.79 |
| Standard deviation $\sigma$ ($10^{-4}$ K$^{-1}$) | 0.30 | 0.54 | 0.31 |

## III. RESULTS

### A. Sample heating

Figure 2 displays the recorded development of the sample temperature when pumping the sample. A temperature jump exceeding 100 K is observed. After about 500 ps, the observed temperature slowly decreases again.

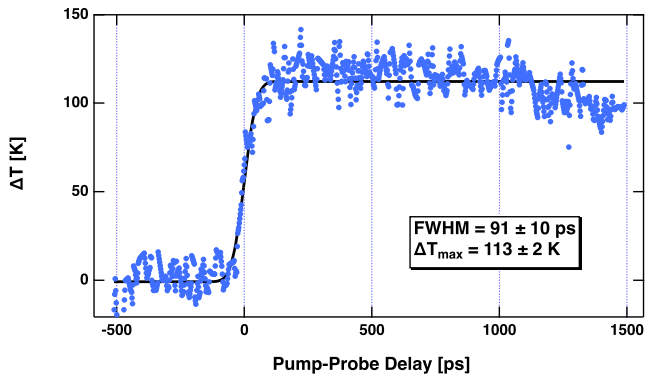


**FIG. 2.** Temperature transient of the Au film as extracted from the reflectivity changes. The data are fitted by Eq. (3). The point of zero delay is extracted from the fit ($t_0$).

In order to quantitatively evaluate the data, the cumulative distribution function, *cdf*, was used,

$$cdf(t) = T_0 + \frac{1}{2}\Delta T_{\max}\left(1 + \int_{t_0'}^{t} \exp\left[-\frac{(t'-t_0')^2}{2\sigma^2}\right]dt'\right), \quad (3)$$

where $T_0$ is the idle temperature of the sample, $\Delta T_{\max}$ is the final temperature increase, and $t_0'$ is the midpoint in the increase (for a general discussion of laser-induced heat transport, consult Ref. 19). Fitting the data yields values of 113 ± 2 K for $\Delta T_{\max}$ and 91 ± 10 ps for the full width at half maximum (FWHM = $2\sqrt{2\ln 2}\,\sigma$) of the Gaussian heat transfer underlying the temporal profile. The latter must be compared to the duration of the heating laser pulse of 19 ps (FWHM). This broadening by a factor larger than three needs to be explained. The penetration depth for 532 nm light is ~13 nm in Ti and ~20 nm in Au. Hence, the heating light is predominantly absorbed in the Ti film. Ti has also the larger electron–phonon coupling constant, $G$.[20,21] Hot electron diffusion in the two-layer system[6] and heat conduction transport energy to the surface[5,22] eventually result in thermal equilibration. As the temperature is measured optically from the front side and the penetration length is smaller than the Au film thickness, the measurement will sample the temperature effect on the top 10–20 nm. The fitted curve will be regarded as representing the temperature of the bath of lattice vibrations with which adsorbed molecules are interacting.

### B. vSF spectra at elevated temperatures

Figure 3 displays the vSF spectrum of the symmetric stretch ($\nu_s$) of the $NO_2$ group of 4-NTP at various sample temperatures established by static heating (top) and recorded at different delay times between the heating pump pulse and SF probe pulse pair

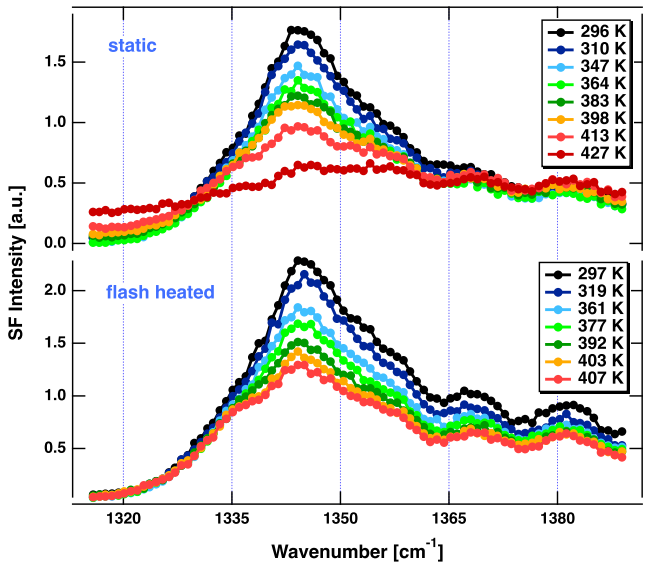


**FIG. 3.** vSF spectra of 4-NTP, recorded in *ppp* at various elevated temperatures, when the sample is heated using a conventional static heater (top panel) and by means of a laser pump pulse (bottom panel). In the latter case, the temperatures were inferred from the concurrent measurement of the reflectivity.

(bottom). In the latter case, the datasets are labeled by the temperature values that the concurrent reflectivity measurement suggests as temperature for that delay. The ($\nu_s$) mode at 1342 cm$^{-1}$ is spectroscopically isolated from the CH stretching modes around 3000 cm$^{-1}$, and the C–C stretches in the range of 1540 to 1600 cm$^{-1}$, belonging to the phenyl ring. The anti-symmetric stretch, which is found at 1530 cm$^{-1}$, carries very low intensity in vSFS. The dips in the spectral profile at 1340, 1363, and 1375 cm$^{-1}$ are due to IR light absorption by the moisture in ambient air. Attempts to correct the spectra turned out to be futile in view of the dependence on varying levels of humidity and unnecessary in view of the generally large error margins when fitting the *ssp* spectra. In the static experiment, a decrease in the intensity of the vibrational band was observed with increasing temperature. The peak intensity decreases at the beginning almost linearly with temperature until, starting from 400 K, the feature rapidly becomes unresolvable. At 400 K, only 65% of the initial peak intensity is observed.

### C. Flash heating

In the laser-heated experiment (Fig. 4), the development of the spectra with temperature is qualitatively rather similar. We regard the differing absolute intensity as an experimental artifact, likely due to slightly different experimental conditions. However, a detailed inspection reveals the dynamics we are interested in.

Further insight is obtained when examining the evolution of the molecular peak intensity as a function of the pump–probe delay. To this end, the time-dependent spectra were fit using Eq. (1), and the obtained parameters are displayed in Figs. S2 and S3. From the fit parameters, we calculate the molecular intensity, $I_{mol} = (A/\Gamma)^2$, in order to isolate the molecular response from one of the combined NTP/Au system (Fig. 5). $I_{mol}$ is the fictive intensity one would observe if the non-resonant background were not present. In order

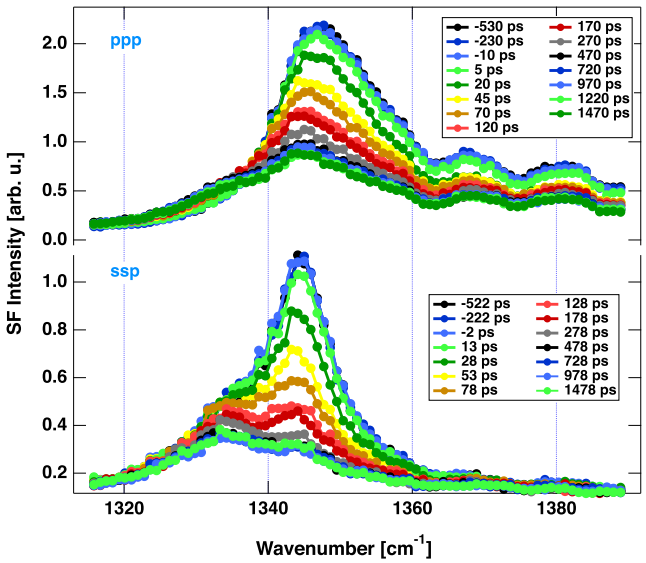


**FIG. 4.** vSF spectra of 4-NTP, recorded using the *ppp* (top) and *ssp* (bottom) polarization combinations at different delays between the pump and probe. The indicated delays have been calibrated by fitting the data shown in Fig. 5.

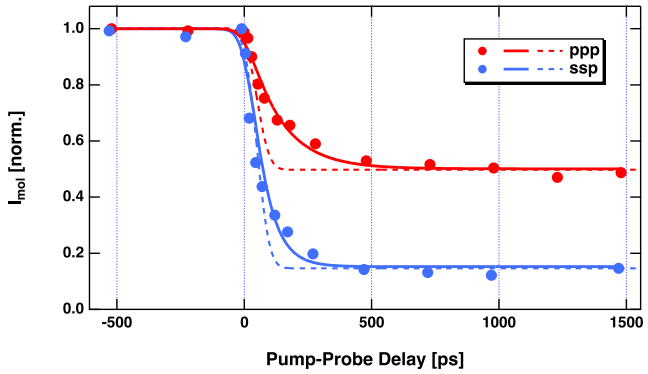


**FIG. 5.** Evolution of the molecular SF intensity (in *ppp* and *ssp*) as a function of the pump–probe delay. The molecular intensity is obtained by fitting the time-dependent spectra and normalizing the values to the ones at negative delays. Depicted is further what would be predicted if the attenuation followed the evolution of the surface temperature as experimentally determined by the reflectivity measurement (dashed lines). The solid lines are fits using the model formulated in Eq. (4). The fit results are listed in Table II.

to connect these transients to the temporal evolution of the surface temperature, we employed the fit curve derived above (Fig. 2) and the observation that the reflected intensity decreases linearly with temperature over the range of temperatures studied. Hence, it is only necessary to scale the curve to the maximum attenuation observed for large delays. It is evident that this prediction does not represent the data well. Even if one allows for slight non-linearity in the temperature dependence of the molecular intensity, the discrepancy persists. It is, therefore, concluded that a time lag must exist between the surface temperature rise and the local temperature that governs the molecular intensity.

As we have seen that the reduction in reflectivity is a good linear proxy of the surface temperature, we can directly use this quantity. On the other end, we saw that the peak intensity of the molecular signal decreased linearly with the substrate temperature. Hence, we can directly formulate a two-temperature model using the reflectivity, $R_{sub}$, and molecular intensity, $I_{mol}$,

$$\mathrm{d}I_{mol} = \left(B\,R_{sub} - I_{mol}\right)\frac{1}{\tau}\,\mathrm{d}t, \tag{4}$$

where $B$ serves to scale the temperature effects on the two quantities. $\tau$ is the time constant for the equilibration in temperatures between the substrate and molecular spectral intensity of the $\nu_s$ mode of 4-NTP.

By integrating this differential equation, we obtain the curve to fit the data. The cdf fit curve displayed in Fig. 2 is used for $R_{sub}$ as a function of time. The fit indicates for the time constant $\tau$ a value of 130 ± 23 ps when using the *ppp* data. Evaluating the *ssp* data, we obtain 62 ± 21 ps (Table II). Thus, first of all, the response by the molecular intensity is significantly delayed with respect to the temperature rise at the surface, and second, the time lag appears to differ by a factor of 2 when probing with different polarization combinations. The latter effect is too large to be explained by experimental uncertainties. The observation may at first glance be irreconcilable, given that the molecule and substrate are identical in both cases and

**TABLE II.** Compilation of fit results and errors (confidence interval = 1$\sigma$) of the profiles in Fig. 5 to Eq. (4). *R* was inferred from the cdf fit curve to the reflectivity measurement (s. Fig. 2).

| | $\tau$ (ps) | $B_0$ | $t_0$ (ps) |
|---|---|---|---|
| *ppp* | 130 ± 23 | 0.50 ± 0.01 | 0 ± 11 |
| *ssp* | 62 ± 21 | 0.42 ± 0.02 | 0 ± 14 |

we probe at the identical vibrational mode. It is also noteworthy that this observation corroborates that the signal attenuation cannot be attributed to the excitation of the vibration itself by, e.g., a hot electron scattering mechanism, as the population of the vibrationally excited states would influence the molecular intensity in both polarization combinations to an identical extent.

It needs, however, to be recalled that the *ppp* and *ssp* polarization combinations probe different components of $\chi^{(2)}$, which is a 3rd rank tensor. Hence, a more detailed examination of the equations that describe the components of $\chi^{(2)}$ is warranted. The theory connecting $\chi^{(2)}$ to the amplitudes, *A*, governing the spectrum and the considerations of the restriction that molecular symmetries impose on the individual components shall not be repeated here again. For detailed discussions, the reader is referred to the seminal work by Shen,[1,23] Hirose *et al.*,[24,25] and Wang *et al.*[26]

## IV. DISCUSSION

The tensor components are affected to varying extents by shifts in the mean tilt angle of the symmetry axis of the group probed with respect to the surface normal and its distribution around the mean value. In the case of 4-NTP, the group's and the molecule's symmetry axes are identical. In previous work,[13] we found that 4-NTP preferentially adsorbs in a 2 × 2 structure with a mean tilt angle of about 50°, in which case the anchoring sulfur atoms are 8 Å apart. Note that local probe experiments indicate that 4-NTP monolayers exhibit well-ordered domains coexisting with areas of flat lying molecules.[27] However, we will continue the discussion ignoring the latter domains, as the molecules in these are not expected to contribute significantly to the vSF signal of the $NO_2$ $\nu_2$ stretch.

It is straightforward to deduce $\chi^{(2)}_{zzz}$ and $\chi^{(2)}_{xxz}$ as a function of delay from the recorded *ssp* and *ppp* data (Fig. 6). The *ssp* data are only dependent upon $\chi^{(2)}_{yyz}$, while the *ppp* data are dependent upon $\chi^{(2)}_{zzz}$ and $\chi^{(2)}_{xxz}$. $\chi^{(2)}_{yyz}$ and $\chi^{(2)}_{xxz}$ have identical values in achiral, azimuthally isotropic systems. As is common practice, we neglect the contribution of the tensor components $\chi^{(2)}_{xzx}$ and $\chi^{(2)}_{zxx}$ to the *ppp* intensity, as they are small on metal substrates[3] (see also the supplementary material for calculated values) and partially cancel out when the molecule is not in resonance with either the upconversion or SF light.[26,28] Two of the equations discussed in the review by Wang *et al.*[29] [s. Eq. (24)] can be used to setup a system of two equations with $\chi^{(2)}_{zzz}$ and $\chi^{(2)}_{yyz}$ as only unknowns. The material constants that one needs to know and the values used are given in Table S2. A fit to the $\chi^{(2)}_{xxz}$ data indicates a time lag of 83 ± 21 ps with respect to the surface temperature transient. The value lies in between the two obtained when evaluating the molecular intensities. The data for

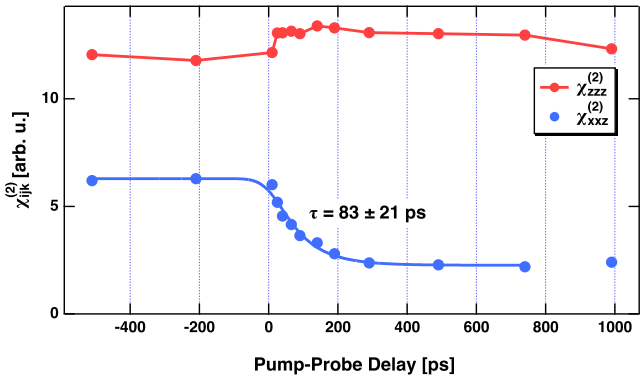


**FIG. 6.** $\chi^{(2)}_{zzz}$ and $\chi^{(2)}_{xxz}$ as function of pump–probe delay. $\chi^{(2)}_{xxz}$ and $\chi^{(2)}_{yyz}$ are identical. The blue solid lines are a fit using the model formulated in Eq. (4) to the $\chi^{(2)}_{xxz}$ data point.

$\chi^{(2)}_{zzz}$ are rather noisy, but if it carries any information at all, a rapid increase to a 10% larger value is indicated. Inspecting the fit curves closer, it is noted that the quality of the fit to $\chi^{(2)}_{xxz}$ is better when compared to the one to the *ssp* molecular intensities.

Figure 7 displays the calculated dependencies of the two tensor components of interest as a function of tilt angle for different widths of the distribution in that quantity. Note that an increase of $\chi^{(2)}_{zzz}$ is consistent with the calculation for a widening of the distribution, provided the mean tilt angle is larger than 40°, a claim that is supported by earlier experiments. On the other hand, in this scenario, $\chi^{(2)}_{xxz}$ is expected to decrease, as just suggested by our data evaluation.

This finding allows us to also understand the difference in the time evolution between the *ssp* and *ppp* spectra. It arises because the ensemble averages over $\chi^{(2)}_{zzz}$ and $\chi^{(2)}_{xxz,yyz}$ evolve differently in time. However, the latter is by the end not surprising as these two tensor components have different dependencies on the mean tilt angle and the width of the distribution around it. Closer inspection of Fig. 7

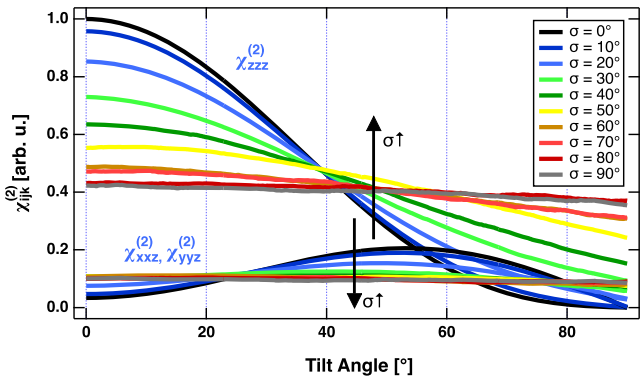


**FIG. 7.** Calculated dependence of $\chi^{(2)}_{zzz}$ and $\chi^{(2)}_{xxz}$ on the tilt angle for a range of assumed distributions with varying widths. The vertical arrows indicate the direction in which $\chi^{(2)}_{ijk}$ shifts if the spread in tilt angles increases.

reveals that $\chi^{(2)}_{xxz,yyz}$ rapidly decreases as the mean tilt angle increases, starting from its room temperature value of about 50° and a moderate width. An increase in width enlarges this effect. In contrast, for $\chi^{(2)}_{zzz}$ the effect of an increased mean tilt angle is at least partially compensated by the effect of an increase in width. Hence, when the structural change has developed to some extent, the effect on $\chi^{(2)}_{xxz,yyz}$ may be more pronounced than the one on the sum of $\chi^{(2)}_{xxz,yyz}$ and $\chi^{(2)}_{zzz}$. For the temporal evolution, it is important to note that the developments are not linear in tilt angle change. Hence, it would be odd if the two apparent time constants derived from the *ssp* and *ppp* spectra were not different. The time constant representing the microscopic processes could only be determined by modeling the evolution of the structure of the adlayer. Hence, we restrict ourselves to conclude that the time lag with respect to the substrate temperature rise is about 100 ps.

If one wants to assess the interplay between possible shifts in the mean tilt angle and the widening of the distribution, a detailed discussion of the observed intensity changes *and* the shift in the ratio of the *ssp* to *ppp* molecular intensities is necessary. This enables the formulation of the constraints that can be inferred from the data (for details, consult the supplementary material). It is found that the mean tilt angle increases from the $50° \pm 8°$ observed for the cold sample with a rather narrow distribution reflected by $\sigma = 8° \pm 8°$. The heated sample exhibits a very wide distribution of tilt angles centered around $80° + 7°/-8°$. This suggests an interpretation that the initially well-ordered domains on the surface break up as the molecules adsorb heat. Having overcome the attractive intermolecular interaction resulting from the stacking of the phenyl rings, the molecules carry out large amplitude pendulum motions. It is, therefore, preferable to refer to this process as disordering rather than reorientation. Such a scenario is likely because the well-ordered domains are already small to begin with and coexist with less densely packed domains, indicating an intermolecular interaction too weak to coerce a perfect crystalline assembly, leaving plenty of available space for molecules that want to break out of order. However, the loss of order must be recovered within the 7 s that elapse before the same spot is tested again on the constantly rotating sample, as we observe the vSF signal returning to its original level.

It needs to be pointed out that the quantitative analysis involved material constants (see the supplementary material) that are only known with poor accuracy, in particular the refractive index of the adlayer, $n_{Ad}$. We tested a range of values from the literature ($n_{Ad}$ between 1.2 and 1.65) and found that the qualitative conclusion just discussed is supported by everyone. For example, the mean tilt angle for room temperature becomes 66°, and the distribution after flash-heating spreads over a narrower range of angles from flat-lying to somewhat uptilted for $n_{Ad} = 1.2$ when compared to $n_{Ad} = 1.62$.

When comparing our results with the work of Dlott and coworkers,[10,30] it is important to note that we heat the substrate much more slowly by using a contact layer of 13 nm Ti instead of 0.8 nm Cr. The consequence is not only that the light is predominantly absorbed in this contact layer but also that the interaction of hot electrons with the SAM is less likely since the electron–phonon coupling constant of the *d*-band metal Ti is larger than that of the noble metal Au. Furthermore, the lifetime of hot electrons is short compared to the 20 ps laser pulse length utilized here and the expected lifetime of $NO_2$ valence vibrations. Therefore, the density of these is further spread out in time when compared to the 200 fs heating experiments by Dlott *et al.* Finally, the somewhat longer wavelength, 532 nm instead of 400 nm, used for flash-heating also reduces electronic effects. Moreover, thermal excitations of the $NO_2$ mode will not be significant, as for these to be significant, the temperature remains too low. For that reason, we do not observe the overshoot in the response at short delays, neither in the surface reflectivity nor in the transients of the vSF signal attenuation. Thus, we are able to study the isolated heat transfer due to the interaction with the lattice vibrations of the Au substrate. Having collected spectra using the *ssp* and *ppp* polarization combinations allows us to analyze the adsorption geometry of the molecules in this state. The analysis indicates that the ordered structure is largely broken up. The time-resolved data indicate that the spread of disorder in the SAM evolves with a time lag of 100 ps with respect to the substrate temperature.

In parallel with the loss of intensity, we observe a shift in the center frequency and a broadening of the line (for details, see the supplementary material). These are effects that were discussed in detail by Berg *et al.*[31] and attributed to interactions with lower wavenumber deformation modes within the molecule. Our observations are in line with this work.

## V. SUMMARY

The response of a monolayer of 4-nitrothiophenol adsorbed on a thin Au film to flash heating was studied. A 19 ps laser pulse with a wavelength of 532 nm was directed onto the backside of a 13 nm Ti/30 nm Au structure to induce the heating. Within 91 ps, the temperature of the sample increased by 113 K from room temperature. Vibrational sum frequency spectroscopy was used to characterize the adsorption geometry of the molecules in the ordered domains in the monolayer film. Upon heating, the initially ordered monolayer largely lost its structure. While the molecules are initially tilted by about 50° with respect to the surface normal, the analysis indicates that the mean tilt angle increases to 80° with a spread for individual molecules of up to a tilt angle of 40° upon heating. The evolution of this loss of order lags about 100 ps behind the temperature rise of the substrate.

## SUPPLEMENTARY MATERIAL

See the supplementary material for details on the analysis of the vSF spectra.

## DEDICATION

This work was dedicated to Yuen-Ron Shen.

## ACKNOWLEDGMENTS

E.H. acknowledges the funding by the Deutsche Forschungsgemeinschaft (DFG, German Research Foundation) Project No. 278162697 within the CRC 1242 "Non-Equilibrium Dynamics of Condensed Matter in the Time-Domain." We thank Dana Dlott for generously sharing with us a glass/Cr/Au substrate when we first started this study. We thank Nelli Kremer and Tim Lämmerzahl for their valuable discussions and acknowledge the support during the initial stages of the experiment by Damian Firla and Andre Beier-Hannweg.

## AUTHOR DECLARATIONS

### Conflict of Interest

The authors have no conflicts to disclose.

### Author Contributions

**Matthias Linke**: Data curation (equal); Formal analysis (equal); Investigation (equal); Software (equal); Writing – original draft (equal). **Joshua Multhaup**: Investigation (equal); Software (equal). **Eckart Hasselbrink**: Conceptualization (equal); Funding acquisition (equal); Project administration (equal); Validation (equal); Writing – original draft (equal); Writing – review & editing (equal).

## DATA AVAILABILITY

The data that support the findings of this study are available from the corresponding author upon reasonable request.

## REFERENCES

[1]Y. R. Shen, "Surface properties probed by second-harmonic and sum-frequency generation," Nature **337**, 519–525 (1989).
[2]C. S. Tiana and Y. R. Shen, "Recent progress on sum-frequency spectroscopy," Surf. Sci. Rep. **69**, 105 (2014).
[3]A. G. Lambert, P. B. Davies, and D. J. Neivandt, "Implementing the theory of sum frequency generation vibrational spectroscopy: A tutorial review," Appl. Spectrosc. Rev. **40**, 103 (2005).
[4]Y.-R. Shen, *Fundamentals of Sum-Frequeuency Spectroscopy* (University Press, Cambridge, 2016).
[5]D. Tzou and K. Chiu, "Temperature-dependent thermal lagging in ultrafast laser heating," Int. J. Heat Mass Transfer **44**, 1725–1734 (2001).
[6]M. Heckschen, Y. Beyazit, E. Shomali, F. Kühne, J. Jayabalan, P. Zhou, D. Diesing, M. E. Gruner, R. Pentcheva, A. Lorke, B. Sothmann, and U. Bovensiepen, "Spatio-temporal electron propagation dynamics in Au/Fe/MgO(001) in nonequilibrium: Revealing single scattering events and the ballistic limit," PRX Energy **2**, 043009 (2023).
[7]M. Horn-von Hoegen, "Structural dynamics at surfaces by ultrafast reflection high-energy electron diffraction," Struct. Dyn. **11**, 021301 (2024).
[8]Z. Wang, J. A. Carter, A. Lagutchev, Y. K. Koh, N.-H. Seong, D. G. Cahill, and D. D. Dlott, "Ultrafast flash thermal conductance of molecular chains," Science **317**, 787 (2007).
[9]J. A. Carter, Z. Wang, and D. D. Dlott, "Ultrafast nonlinear coherent vibrational sum-frequency spectroscopy methods to study thermal conductance of molecules at interfaces," Acc. Chem. Res. **42**, 1343–1351 (2009).
[10]C. M. Berg, A. Lagutchev, and D. D. Dlott, "Probing of molecular adsorbates on Au surfaces with large-amplitude temperature jumps," J. Appl. Phys. **113**, 183509 (2013).
[11]W. Mar and M. L. Klein, "Molecular dynamics study of the self-assembled monolayer composed of $S(CH_2)_{14}CH_3$ molecules using an all-atoms model," Langmuir **10**, 188 (1994).
[12]Y. Zhang, G. L. Barnes, T. Yan, and W. L. Hase, "Model non-equilibrium molecular dynamics simulations of heat transfer from a hot gold surface to an alkylthiolate self-assembled monolayer," Phys. Chem. Chem. Phys. **12**, 4435 (2010).
[13]J. Hekele, M. Linke, T. Keller, J. Jose, M. Hille, E. Hasselbrink, S. Schlücker, and P. Kratzer, "A fresh look at the structure of aromatic thiols on Au surfaces from theory and experiment," J. Chem. Phys. **155**, 044707 (2021).
[14]M. Buck and M. Himmelhaus, "Vibrational spectroscopy of interfaces by infrared–visible sum frequency generation," J. Vac. Sci. Technol., A **19**, 2717–2736 (2001).
[15]F. Vidal and A. Tadjeddine, "Sum-frequency generation spectroscopy of interfaces," Rep. Prog. Phys. **68**, 1095–1127 (2005).
[16]P. E. Ohno, H.-f. Wang, and F. M. Geiger, "Second-order spectral lineshapes from charged interfaces," Nat. Commun. **8**, 1032 (2017).
[17]B. Busson and A. Tadjeddine, "Non-uniqueness of parameters extracted from resonant second-order nonlinear optical spectroscopies," J. Phys. Chem. C **113**, 21895 (2009).
[18]A. Beran, "The reflectance behaviour of gold at temperatures up to 500 °C," TMPM, Tschermaks Mineral. Petrogr. Mitt. **34**, 211 (1985).
[19]D. Bäuerle, *Laser Processing and Chemistry*, 4th ed. (Springer, Heidelberg, 2011), Chap. 2.2.
[20]M. Bauer, A. Marienfeld, and M. Aeschlimann, "Hot electron lifetimes in metals probed by time-resolved two-photon photoemission," Prog. Surf. Sci. **90**, 319 (2015).
[21]M. Volkov, S. A. Sato, F. Schlaepfer, L. Kasmi, N. Hartmann, M. Lucchini, L. Gallmann, A. Rubio, and U. Keller, "Attosecond screening dynamics mediated by electron localization in transition metals," Nat. Phys. **15**, 1145–1149 (2019).
[22]T. Qiu and C. Tien, "Femtosecond laser heating of multi-layer metals—I. Analysis," Int. J. Heat Mass Transfer **37**, 2789–2797 (1994).
[23]Y. R. Shen and V. Ostroverkhov, "Sum-frequency vibrational spectroscopy on water interfaces: Polar orientation of water molecules at interfaces," Chem. Rev. **106**, 1140–1154 (2006).
[24]C. Hirose, N. Akamatsu, and K. Domen, "Formulas for the analysis of the surface SFG spectrum and transformation coefficients of cartesian SFG tensor components," Appl. Spectrosc. **46**, 1051–1072 (1992).
[25]C. Hirose, N. Akamatsu, and K. Domen, "Formulas for the analysis of surface sum-frequency generation spectrum by CH stretching modes of methyl and methylene groups," J. Chem. Phys. **96**, 997–1004 (1992).
[26]H.-F. Wang, W. Gan, R. Lu, Y. Rao, and B.-H. Wu, "Quantitative spectral and orientational analysis in surface sum frequency generation vibrational spectroscopy (SFG-VS)," Int. Rev. Phys. Chem. **24**, 191 (2005).
[27]J. U. Nielsen, M. J. Esplandiu, and D. M. Kolb, "4-Nitrothiophenol SAM on Au(111) investigated by in situ STM, electrochemistry, and XPS," Langmuir **17**, 3454 (2001).
[28]X. Li and G. Rupprechter, "A modeling analysis of molecular orientation at interfaces by polarization-dependent sum frequency generation vibrational spectroscopy," Chin. J. Catal. **40**, 1655–1667 (2019).
[29]H.-F. Wang, L. Velarde, W. Gan, and L. Fu, "Quantitative sum-frequency generation vibrational spectroscopy of molecular surfaces and interfaces: Lineshape, polarization, and orientation," Annu. Rev. Phys. Chem. **66**, 189 (2015).
[30]J. A. Carter, Z. Wang, H. Fujiwara, and D. D. Dlott, "Ultrafast excitation of molecular adsorbates on flash-heated gold surfaces," J. Phys. Chem. A **113**, 12105 (2009).
[31]C. M. Berg, Y. Sun, and D. D. Dlott, "Temperature-dependent dynamic response to flash heating of molecular monolayers on metal surfaces: Vibrational energy exchange," J. Phys. Chem. B **118**, 7770–7776 (2013).